Fusion Engineering and Design 98–99 (2015) 1638–1642

Contents lists available at ScienceDirect

Fusion Engineering and Design

journal homepage: www.elsevier.com/locate/fusengdes

The "ductility exhaustion" method for static strength assessment of fusion structures

Vaughan Thompson*, Zsolt Vizvary

CCFE, Culham Science Centre, Abingdon OX14 3DB, UK

HIGHLIGHTS

- Reduced conservatism and more complex geometry.
- Assessment process simplified.
- Gives insight into real material behaviour – virtual proof test.
- Leads onto structural failure modelling.
- Ductility exhaustion and global plastic collapse structural assessment.

GRAPHICAL ABSTRACT

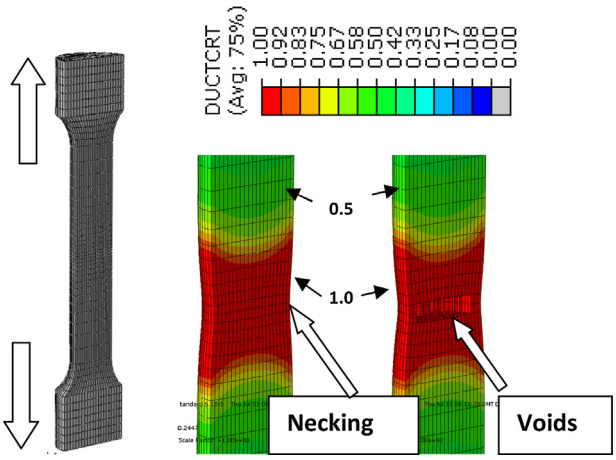

ARTICLE INFO

Article history:
Received 25 September 2014
Received in revised form 9 June 2015
Accepted 9 June 2015
Available online 23 June 2015

Keywords:
Plasticity
JET
Beryllium
Ductility
Disruption
Abaqus
ANSYS
Limiter

ABSTRACT

The traditional method for static strength assessment of structures uses elastic stresses computed along critical ligaments and then divided into categories depending on their nature e.g. bending/membrane and primary/secondary. More recently, highly realistic plastic simulations are possible using FE (finite elements) which offer useful advantages over the traditional approach including (a) more accurate modelling of complex geometries, (b) a more straightforward assessment process and (c) a less conservative approach. The plastic analysis must consider both global and local effects, and the paper looks in detail at the "ductility exhaustion" method for the latter. Simple test cases show how the method can be applied in both the Abaqus and ANSYS FE Codes and for the case of a JET beryllium tile, the method has improved reserve factors for disruption loads considerably to the point where the lower operating temperature can be safely lowered from 200 °C to 100 °C where the low ductility of beryllium is an issue.

1. Introduction

In traditional structural analysis stresses are linearized along a through-thickness *stress line* so that the components can be separated and assessed, Fig. 1. The stress line represents a potential

* Corresponding author. Tel.: +44 01235 464597.
E-mail address: vaughan.thompson@ccfe.ac.uk (V. Thompson).

http://dx.doi.org/10.1016/j.fusengdes.2015.06.035
0920-3796/

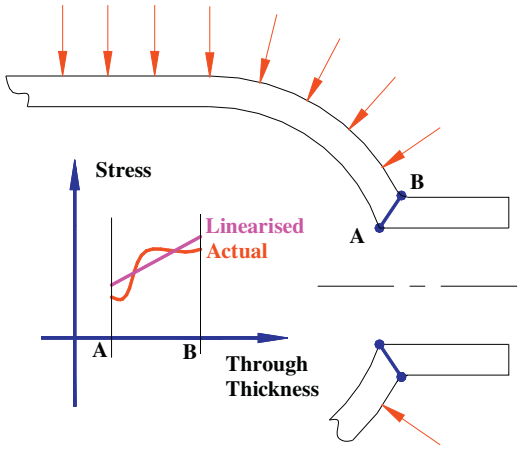

Fig. 1. Linearized stress line.

failure surface in this simple axis-symmetric case and here is both simple to apply and not overly conservative.

The method is often extended to more complex structures such as used in fusion devices. Here, FE codes typically provide the elastic stresses and stress line result, but the choice of stress lines can be labour intensive and the results overly conservative.

2. Plastic analysis

Over recent years, FE codes and desktop computing have advanced to the point where analysts can perform much more advanced structural modelling. In particular, plastic analysis can accurately capture the behaviour of complex structures made from ductile materials and predict when failure will occur.

The process must include both global plastic collapse and local plastic failure, Fig. 2. The maximum deflection versus load characterizes the global behaviour with the failure point defined where the stiffness has fallen to half its initial value. Other definitions exist, but this *half-stiffness* method has the advantage of computation simplicity.

Fig. 2 also shows the local failure line or ductility ratio which is the applied strain divided by the available strain (generally the elongation at failure). Note that in this context, strain refers to *equivalent plastic* strain which is readily computed with FE codes. Local failure occurs when the ductility ratio reaches 1.0 and knock-down factors applied to both local and global failure to give a safe working load to complete the assessment. Recent issues of [1], provide these knock-down factors for a range of pressure vessels materials and guidance for more general materials.

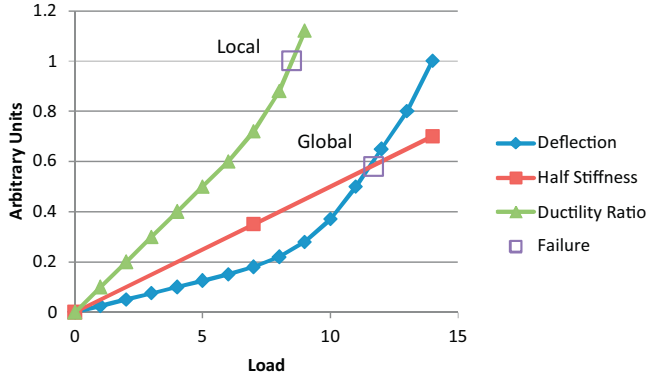

Fig. 2. Local and global failure.

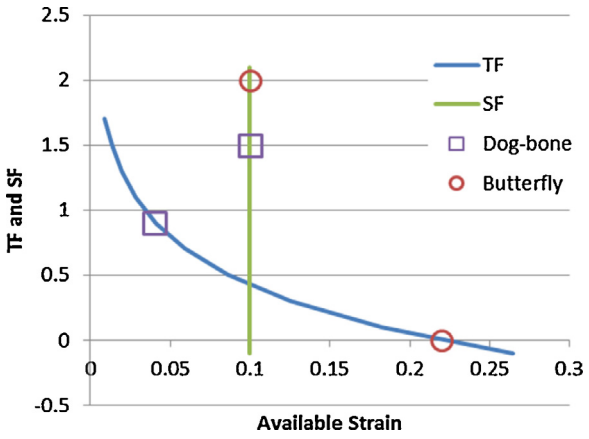

Fig. 3. Local failure strains.

Ref. [1] also shows how to compute the available strain based on the TF (Triaxiality Factor or ratio of mean tension to Von Mises stress). Fig. 3 shows an example with TF plotted against available strain. This example is based on beryllium at 100 °C as described later and uses the measured elongation from *dog-bone* tensile tests along with other material constants conservatively estimated from [1]. Note how the available strain falls with increasing TF which quantifies the vulnerability of structures with high local tension to local failure: in contrast to the traditional approach where local tension and compression are equally treated.

The figure includes the TF from the centre of a dog-bone sample as described later. Here there is tension in all directions with the TF close to 1.0 and tension induced void formation and coalescence characterize the local failure.

In addition to this *tension-induced* mode, local failure through *shear band formation* as described by Li et al. [2] is possible. Fig. 3 includes a simplified example where the local shear failure is based on the SF (Shear Factor) which is a measure of the shear stress independent of the TF as described in [3]. The butterfly test, described later, is designed to exercise shear band failure without tensile failure and Fig. 3 includes SF and TF for both test types. In the dog-bone test the available strain for tension is lower than for shear and so local failure by tension dominates. In the butterfly test the situation is reversed and so local failure by shear dominates.

3. FE analysis of local failure

3.1. Abaqus

The Abaqus FE code, [3], includes advanced material models that readily accommodate local failure and these have been tested using the two cases above.

Fig. 4 shows the dog-bone case which uses a 3D model with one symmetry plane employing reduced integration eight-noded hexahedral elements. The material is set for beryllium at 100 °C as used in the JET case below. The left hand image shows the full model which is pulled axially using controlled displacement. The deformed plots show contours of ductility ratio (DUCTCRT in Abaqus) and illustrate the onset of local failure in the centre image where local necking has started and there is a significant region where the ductility ratio has reached 1. To further exercise the material model, the "failed elements" have had their stiffness ramped to zero and deleted so that the simulation can advance into the formation and coalescence of voids as illustrated on the right. Taking the model to *failure* illustrates the accuracy of the modelling, can be useful when fitting material constants to tensile test results,

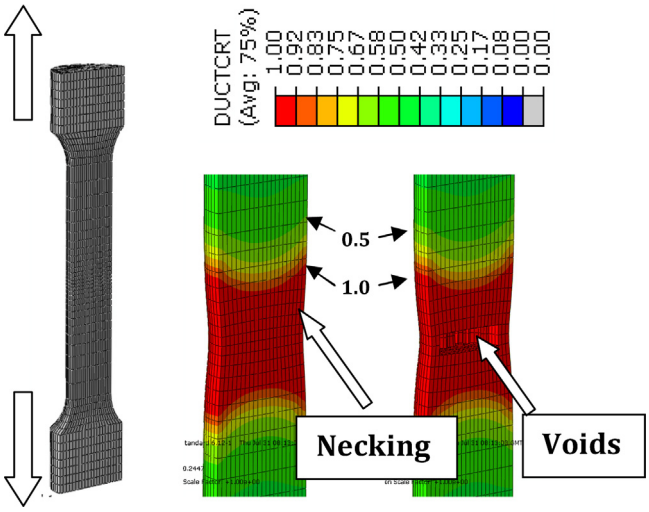

Fig. 4. Failure ratio in dog-bone tensile test.

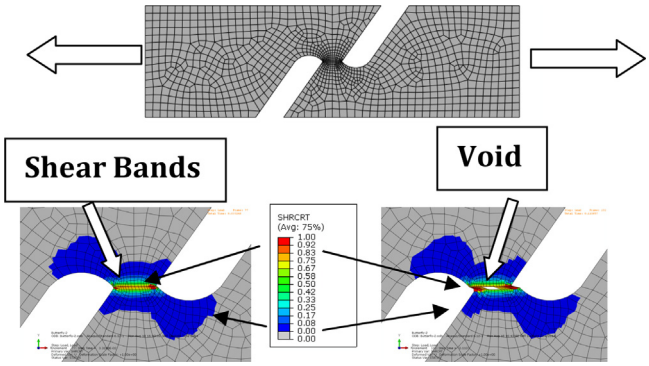

Fig. 5. Failure ratio in butterfly shear test.

and when simulating structural failure scenarios such as in accident conditions.

Fig. 5 shows the results of a "butterfly" test which consists of a 2-D plane stress simulation of a thin plane sculpted to produce a shear-loaded ligament.

Again the analysis uses reduced integration linear elements to improve convergence rates and "kills" the failed elements to reveal the characteristic shear band failure. Options exist within Abaqus to combine both failure modes in a single analysis.

Mesh separation is described in more detail in the ANSYS analysis below.

3.2. ANSYS

The ANSYS FE model replicates the geometry and material properties from the Abaqus case. However ANSYS does not provide the ductility ratio directly. Hence a macro was written to calculate the ductility ratio after each iteration step from the available results: principal and equivalent stresses along with the equivalent plastic strain. To speed up the process first order elements were used, but the method is equally applicable to second order elements.

Once the ductility ratios have been computed the analysis used the element birth and death technique available in ANSYS to deactivate the failed elements. "Killing" these elements means that their stiffness is reduced but the elements are still present.

The results show a similar necking and void formation as in Abaqus (Fig. 6).

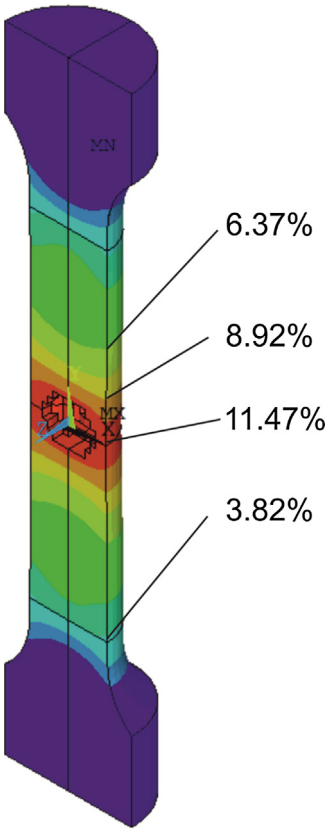

Fig. 6. Equivalent plastic strain in dog-bone tensile test.

The displacement load was applied in 20 increments and Fig. 7 shows snapshots of the ductility ratio and equivalent plastic strain at each time step.

The major steps of the failure process show how the larger-than-1 ductility ratio region spreads (grey, circled region) and how the equivalent plastic strain evolves with the "dead" elements tuned off.

It may be noticed, Fig. 8, that the analysis obtains the well known *cup and cone* shape at the failure by adding the dead elements to one side of the broken sample (the failed material does not diappear in reality).

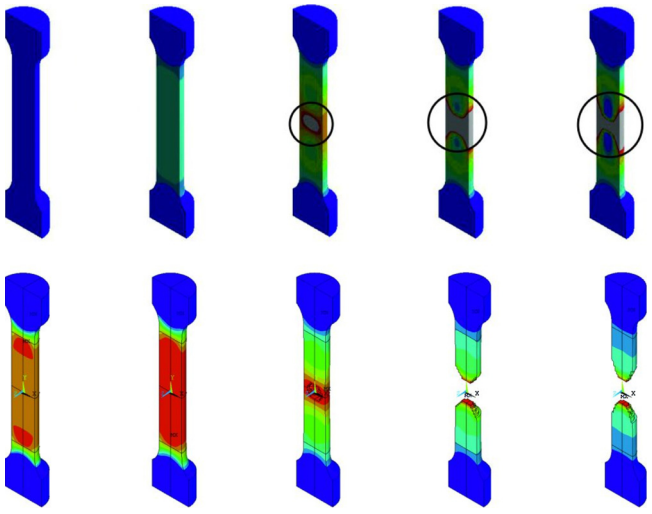

Fig. 7. Ductility ratio and equivalent plastic strain evolution.

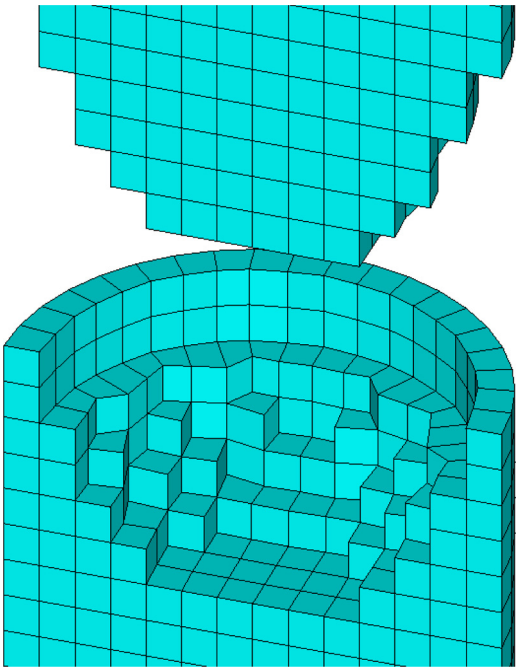

Fig. 8. Typical cup and cone at the end of the test.

4. JET beryllium tile

In 2009, the ILW (Iter-Like Wall) project refurbished the plasma facing surfaces in JET by replacing the existing CFC (Carbon-Fibre reinforced Carbon) tiles with beryllium. The high electrical conductivity and low strength of beryllium at high temperatures was the subject of extensive work during the design phase by Thompson et al. [4], using traditional elastic methods. Fig. 9 shows the critical case: the IWGL (Inner Wall Guard Limiter) wing tile.

This tile is particularly vulnerable to eddy and halo disruption loads which can result in large reactions on the beryllium from the limited abutment provided by the Inconel tile carrier and supporting pin. The results of this work imposed operational limits on JET.

At the time of the earlier analysis, the minimum JET operating temperature of 200 °C was sufficient to ensure sufficient beryllium ductility, see Fig. 10, and the critical case was considered to be a "hot case" at 600 °C.

More recently, operation towards 100 °C – the cold case below – has been considered. Hence the earlier work has been updated using advanced plastic methods to assess the implications of reduced ductility at lower temperatures. The opportunity was also

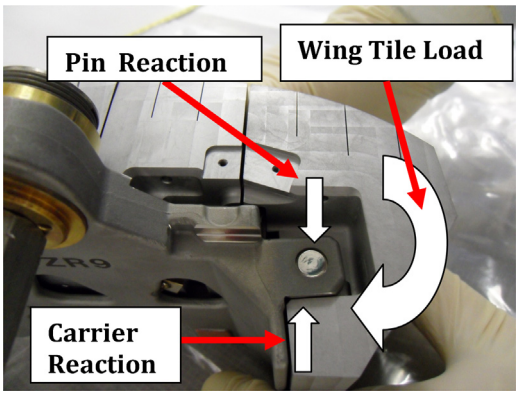

Fig. 9. JET beryllium wing tile.

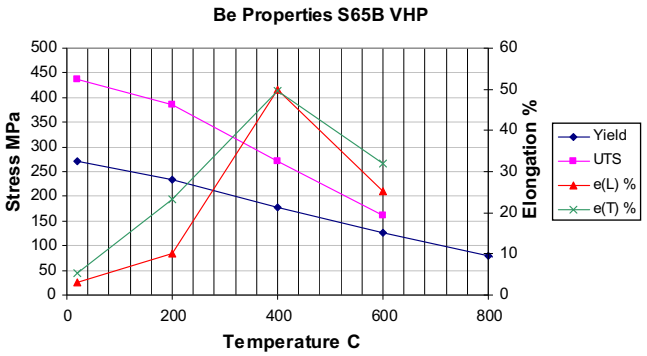

Fig. 10. Mechanical properties of beryllium.

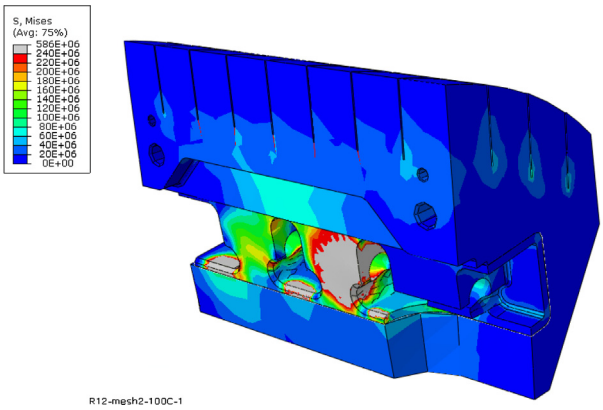

Fig. 11. Wing tile von mises stresses. Cold case.

taken to remove the conservatism imposed by the earlier elastic method which was quite severe in this complex geometry giving an RF (Reserve Factor) of only 0.63 for the JET disruption design case of 6 MA plasma current at 4 T toroidal field (note that present JET operating instructions limit the possible disruption levels to well below this design case).

The updated analysis includes contact between the beryllium wing and the supporting pin and carrier. Fig. 11 illustrates the cold case results with contours of Von Mises stresses in the wing (with the carrier and pin omitted for clarity).

The simulation takes the loads beyond the design case by applying an over-load factor so that failure can be assessed along with a safe load using suitable knock-down factors. Note the grey region

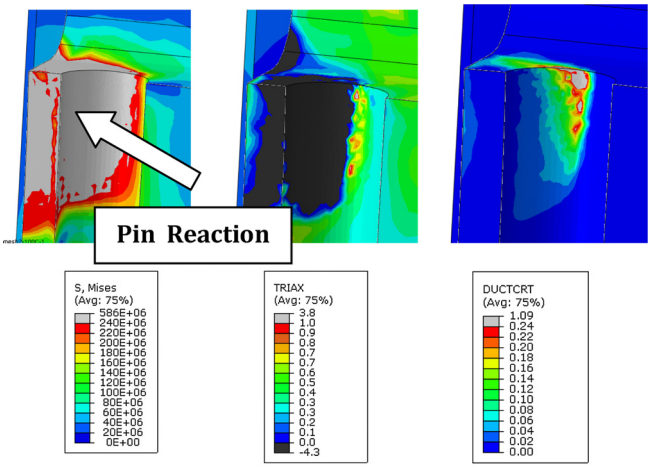

Fig. 12. Be tile local failure. Cold case.

Table 1
JET be tile.

Case	Elongation (%)	Yield, MPa	Failure mode	Reserve factor
Hot, 600 °C	25.2	126	Global	1.8
			Local	5.1
Cold, 100 °C	9.5	229	Global	2.8
			Local	2.9

where contact with the pin results in gross yielding in the beryllium and global failure dominates this case.

Fig. 12 illustrates the results of the cold case where the wing is shown in section with the pin and carrier removed to highlight the local failure which is important in this case. The left view red area shows the high Von Mises stresses due to local reaction with the pin. The centre view gives the TF contours and the black region indicates compression in the pin contact area as expected. The ductility ratio in the right view reflects the apposing effects of high stress and low TF with the critical area being on the edge of the contact area.

Table 1 summarizes the results and shows that the RFs are adequate for both cases with global failure dominating the hot case and global and local failure being comparable for the cold case.

Acknowledgments

This work was carried out within the framework of the European Fusion Development Agreement. For further information on the contents of this paper please contact publications-officer@jet.efda.org. The views and opinions expressed herein do not necessarily reflect those of the European Commission. This work was also part-funded by the RCUK Energy Programme under grant EP/I501045.

References

[1] ASME Boiler and Pressure Vessel Code, ASME, 2013.
[2] H. Li, et al., Ductile fracture: experiments and computation, Int. J. Plast. 27 (2011) 147–180.
[3] Abaqus Analysis Users Manual. Version 6.12.
[4] V. Thompson, et al., Analysis and design of the beryllium tiles for the JET ITER-like wall project, Fusion Eng. Des. 82 (2007) 1706–1712.